

Active IRS-Aided MIMO Systems: How Much Gain Can We Get?

Zeyan Zhuang, Xin Zhang, Dongfang Xu, and Shenghui Song

Dept. of ECE, The Hong Kong University of Science and Technology, Hong Kong

Abstract

Intelligent reflecting surfaces (IRSs) have emerged as a promising technology to improve the efficiency of wireless communication systems. However, passive IRSs suffer from the “multiplicative fading” effect, because the transmit signal will go through two fading hops. With the ability to amplify and reflect signals, active IRSs offer a potential way to tackle this issue, where the amplification energy only experiences the second hop. However, the fundamental limit and system design for active IRSs have not been fully understood, especially for multiple-input multiple-output (MIMO) systems. In this work, we consider the analysis and design for the large-scale active IRS-aided MIMO system assuming only statistical channel state information (CSI) at the transmitter and the IRS. The evaluation of the fundamental limit, i.e., ergodic rate, turns out to be a very difficult problem. To this end, we leverage random matrix theory (RMT) to derive the deterministic approximation (DA) for the ergodic rate, and then design an algorithm to jointly optimize the transmit covariance matrix at the transmitter and the reflection matrix at the active IRS. Numerical results demonstrate the accuracy of the derived DA and the effectiveness of the proposed optimization algorithm. The results in this work reveal interesting physical insights with respect to the advantage of active IRSs over their passive counterparts.

I. INTRODUCTION

With the development of innovative applications, there is an increasing demand for higher data rate, reliability, and energy efficiency in future wireless communication systems. To this end, intelligent reflecting surfaces (IRSs), have been proposed as an energy-efficient way to create a favorable channel between the transmitter and receiver [1], [2]. Specifically, IRSs can reshape the wireless channel and improve the signal quality by reflecting signals through a surface composed of a large number of reconfigurable elements.

Many engaging results have been obtained on the analysis and design of IRS-aided systems such as the IRS-aided multiple-input single-output (MISO) [1] and multiple-input multiple-output (MIMO) channels [3]–[5]. In particular, [3] studied the fundamental limit of IRS-aided point-to-point MIMO systems with perfect channel state information (CSI) at the transmitter, receiver, and IRS. However, in practice, perfect CSI is extremely difficult to obtain for IRS-aided systems, especially in the case of fast-fading channels [6]. As a result, [4] investigated the achievable rate of a large-scale passive IRS-aided MIMO system where only statistical CSI is available at the transmitter and the IRS, by random matrix theory (RMT). The design of the transmit covariance matrix and the phase-shift matrix was also considered.

With either perfect or statistical CSI, the potential gain brought by IRSs is often limited by the “multiplicative fading” of the two-hop channel [7]. To circumvent this issue, a new IRS architecture, namely, active IRS, has recently been proposed in [8]. In particular, equipped with the reflection-type amplifiers (e.g., current-inverting converters), active IRSs can not only reflect the signal to a desired direction, but also amplify the signal with additional power [9]. It is worth mentioning that active IRSs and full-duplex (FD) amplify-and-forward (AF) relays differ in both hardware implementation and transmission modes [1]. Specifically, FD AF relays lead to unavoidable self-interference and processing delay when amplifying the received signal. In contrast, active IRSs can amplify signals instantaneously without introducing self-interference, although the processing freedom is limited, i.e., the diagonal reflection matrix. Inspired by these advantages, some researchers have investigated the analysis and design of active IRS-aided systems. In particular, [9], [10] compared the performance of active and passive IRS-aided single-input single-output (SISO) systems given the same overall power budget. The authors of [11] investigated the fundamental limits of IRS-aided MISO systems with partial CSI. However, to the best of the authors’ knowledge, the fundamental limits of active IRS-aided MIMO systems are not yet available in the literature.

Motivated by the above works, in this paper, we investigate the active IRS-aided point-to-point MIMO communication system assuming only statistical CSI at the transmitter and the IRS. The objective is to first determine the fundamental limit of the concerned system, i.e., the ergodic rate. Then, based on the evaluation result, we jointly design the transmit covariance matrix and the reflection matrix to maximize the ergodic rate. We achieve the first objective by deriving the deterministic approximation (DA) of the ergodic rate using RMT. As the optimization problem is non-convex, we propose an alternating optimization (AO)-based algorithm to design the optimal

transmit covariance matrix and reflection matrix. Numerical results validate the accuracy of the DA and effectiveness of the proposed algorithm.

The main contributions of this work include:

- We evaluate the ergodic rate of active IRS-aided MIMO systems with only statistical CSI at the transmitter and the IRS. To obtain a more tractable and computationally-efficient form for ease of use in the following optimization, we derive the DA for the ergodic rate.
- We maximize the DA for the ergodic rate by jointly optimizing the transmit covariance matrix and reflection matrix. To tackle the resulting non-convex optimization problem, an AO-based low-complexity suboptimal algorithm is developed.
- We investigate the impact of the dynamic noise introduced by the active IRS and different power allocation policies. Simulation results unveil that the active IRS is effective to tackle the “multiplicative fading” effect and has consistent advantages over the passive one.

The rest of this paper is organized as follows. In section II, we introduce the system model and formulate the problem. In section III, we derive the DA for the ergodic rate. An AO-based algorithm for optimizing the transmit covariance matrix and the reflection matrix is proposed in section IV. Section V gives the numerical results and Section VI concludes the paper. The notations utilized in this paper are listed in the footnote¹.

II. SYSTEM MODEL AND PROBLEM FORMULATION

A. System Model

As shown in Fig. 1, we consider a MIMO system consisting of a base station (BS) equipped with n_t transmit antennas and a user equipped with n_r receive antennas. Due to the blockage of the direct link, an IRS comprising n_l active reflecting elements is utilized to establish an

¹Notations. In this paper, we use boldfaced uppercase letters and lowercase letters to represent matrices and column vectors, respectively. $\Im(a)$ and $\Re(a)$ denote the imaginary and real part of a complex number a , respectively. \mathbb{R}^+ and \mathbb{C}^+ denote the real non-negative axis $\{x \in \mathbb{R} : x \geq 0\}$ and the upper half plane $\{z \in \mathbb{C} : \Im(z) > 0\}$, respectively. Let $j = \sqrt{-1}$. The (i, j) -th element of matrix \mathbf{A} will be denoted as either a_{ij} or $[\mathbf{A}]_{ij}$. $\text{diag}\{\mathbf{a}\}$ denotes the diagonal square matrix whose diagonal entries are elements of vector \mathbf{a} and $\text{diag}\{\mathbf{A}\} = \text{diag}\{a_{ii}; 1 \leq i \leq n\}$ for all $n \times n$ matrix \mathbf{A} . The superscript ‘ H ’ denotes Hermitian transpose operator. $\text{Tr}(\mathbf{A})$ and $\|\mathbf{A}\|$ represent the trace and spectral norm of \mathbf{A} , respectively. $\mathbb{E}[a]$ denotes the expectation of random variable a . Function $(a)^+ = \max\{a, 0\}$. $\xrightarrow{\text{a.s.}}_X$ represents the almost sure convergence under the process X . $\text{supp}(\mu)$ denotes the support of measure μ .

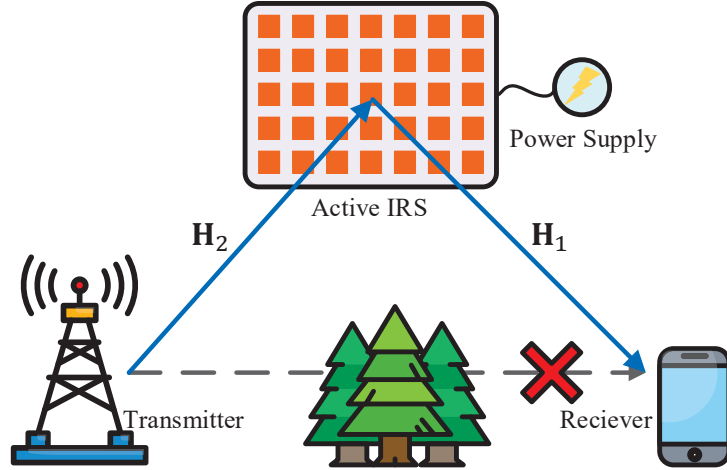


Fig. 1. Active IRS-aided communication system.

alternative communication link. Due to the active nature, the thermal noise introduced during amplification cannot be ignored [8]. Therefore, the received signal \mathbf{y} at the user side is given by

$$\mathbf{y} = \mathbf{H}_1 \Phi \mathbf{H}_2 \mathbf{x} + \mathbf{H}_1 \Phi \mathbf{n}_d + \mathbf{n}_s, \quad (1)$$

where $\mathbf{x} \in \mathbb{C}^{n_t}$ denotes the transmit signal with covariance matrix $\mathbf{Q} = \mathbb{E}[\mathbf{x}\mathbf{x}^H]$. The matrices $\mathbf{H}_2 \in \mathbb{C}^{n_l \times n_t}$, $\mathbf{H}_1 \in \mathbb{C}^{n_r \times n_l}$ represent BS-IRS and IRS-user channel, respectively. The reflection matrix of the active IRS is denoted by $\Phi = \text{diag}\{a_1\phi_1, a_2\phi_2, \dots, a_{n_l}\phi_{n_l}\}$, where $a_i \in \mathbb{R}^+$ and $\phi_i = e^{j\theta_i}$, $i = 1, 2, \dots, n_l$ represent the amplification factor and phase shift of the i -th IRS element, respectively. Different from the passive IRS, a_i can be larger than 1. Here $\mathbf{n}_d \in \mathbb{C}^{n_l}$ denotes the dynamic noise introduced by the active component and $\mathbf{n}_s \in \mathbb{C}^{n_r}$ is the static noise at the receiver. Both \mathbf{n}_d and \mathbf{n}_s are modeled as additive Gaussian white noise (AWGN) [8] [12], i.e., $\mathbf{n}_d \sim \mathcal{CN}(\mathbf{0}, \sigma_d^2 \mathbf{I})$, $\mathbf{n}_s \sim \mathcal{CN}(\mathbf{0}, \sigma_s^2 \mathbf{I})$.

Assuming only statistical CSI at the transmitter and the IRS, the normalized ergodic rate of the channel is given by

$$\begin{aligned} R(\mathbf{Q}, \Phi) = & \frac{1}{n_r} \mathbb{E} \left[\log \det \left(\frac{1}{\sigma_s^2} \mathbf{H}_1 \Phi \mathbf{H}_2 \mathbf{Q} \mathbf{H}_2^H \Phi^H \mathbf{H}_1^H + \frac{\sigma_d^2}{\sigma_s^2} \mathbf{H}_1 \Phi \Phi^H \mathbf{H}_1^H + \mathbf{I} \right) \right. \\ & \left. - \log \det \left(\frac{\sigma_d^2}{\sigma_s^2} \mathbf{H}_1 \Phi \Phi^H \mathbf{H}_1^H + \mathbf{I} \right) \right], \end{aligned} \quad (2)$$

where $R(\mathbf{Q}, \Phi)$ has the unit of bits per second per Hz per antenna. The channel matrix can be written by the Kronecker model as

$$\mathbf{H}_1 = \mathbf{R}_1^{\frac{1}{2}} \mathbf{X}_1 \mathbf{T}_1^{\frac{1}{2}} \quad \text{and} \quad \mathbf{H}_2 = \mathbf{R}_2^{\frac{1}{2}} \mathbf{X}_2 \mathbf{T}_2^{\frac{1}{2}}, \quad (3)$$

where $\mathbf{R}_1 \in \mathbb{C}^{n_r \times n_r}$, $\mathbf{T}_1 \in \mathbb{C}^{n_i \times n_i}$, $\mathbf{R}_2 \in \mathbb{C}^{n_i \times n_i}$ and $\mathbf{T}_2 \in \mathbb{C}^{n_t \times n_t}$ are Hermitian non-negative definite matrices. \mathbf{R}_1 and \mathbf{T}_2 represent the spatial correlation matrices for the receiver and the transmitter, while \mathbf{R}_2 and \mathbf{T}_1 denote the spatial correlation matrices for the IRS. We utilize L_1 and L_2 to denote the path loss for the IRS-user and BS-IRS link, respectively. For ease of manipulation, L_i is absorbed into \mathbf{R}_i . $\mathbf{X}_1 \in \mathbb{C}^{n_r \times n_i}$ and $\mathbf{X}_2 \in \mathbb{C}^{n_i \times n_t}$ are matrices whose entries are independent and identically distributed (i.i.d.) Gaussian random variables (r.v.s) with $[\mathbf{X}_1]_{ij} \sim \mathcal{CN}(0, \frac{1}{n_i})$, $[\mathbf{X}_2]_{ij} \sim \mathcal{CN}(0, \frac{1}{n_t})$. For simplicity, we define

$$\tilde{\mathbf{T}}_1 = \Phi^H \mathbf{T}_1 \Phi \text{ and } \tilde{\mathbf{T}}_2 = \mathbf{Q}^{\frac{1}{2}} \mathbf{T}_2 \mathbf{Q}^{\frac{1}{2}}. \quad (4)$$

Due to the rotational invariance of Gaussian distribution, the normalized ergodic rate can be written as

$$R(\mathbf{Q}, \Phi) = \frac{1}{n_r} \mathbb{E} \left[\log \det \left(\frac{\mathbf{B}_1}{\sigma_s^2} + \mathbf{I} \right) - \log \det \left(\frac{\mathbf{B}_2}{\sigma_s^2} + \mathbf{I} \right) \right], \quad (5)$$

where $\mathbf{B}_1 = (\tilde{\mathbf{H}}_1 \tilde{\mathbf{H}}_2 \tilde{\mathbf{H}}_2^H \tilde{\mathbf{H}}_1^H + \sigma_d^2 \tilde{\mathbf{H}}_1 \tilde{\mathbf{H}}_1^H)$, $\mathbf{B}_2 = \sigma_d^2 \tilde{\mathbf{H}}_1 \tilde{\mathbf{H}}_1^H$, $\tilde{\mathbf{H}}_1 = \mathbf{R}_1^{\frac{1}{2}} \mathbf{X}_1 \tilde{\mathbf{T}}_1^{\frac{1}{2}}$, and $\tilde{\mathbf{H}}_2 = \mathbf{R}_2^{\frac{1}{2}} \mathbf{X}_2 \tilde{\mathbf{T}}_2^{\frac{1}{2}}$.

B. Problem Formulation

Our objective is to optimize the normalized ergodic rate of the active IRS-aided MIMO system under the power constraint at both the transmitter and IRS. The problem can be formulated as

$$\begin{aligned} \mathcal{P}_1 : \quad & \underset{\mathbf{Q} \geq 0, \Phi}{\text{maximize}} \quad R(\mathbf{Q}, \Phi) \\ & \text{s.t.} \quad \text{C1: } \text{Tr}(\mathbf{Q}) \leq n_t P_T, \\ & \quad \quad \text{C2: } \frac{\text{Tr}(\mathbf{Q} \mathbf{T}_2)}{n_t} \text{Tr}(\mathbf{R}_2(\Phi \Phi^H - \mathbf{I})) + \sigma_d^2 \text{Tr}(\Phi \Phi^H) \leq P_A, \end{aligned} \quad (6)$$

where C1 represents the maximum power constraint at the transmitter and C2 denotes the amplification power budget of the active IRS.

Remark 1. The received signal of the active IRS is $\mathbf{s}_{in} = \mathbf{H}_2 \mathbf{x}$ and the reflected signal is $\mathbf{s}_{out} = \Phi \mathbf{H}_2 \mathbf{x} + \Phi \mathbf{n}_d$. The amplification power of the active IRS is $\mathbb{E}[\mathbf{s}_{out}^H \mathbf{s}_{out}]$ [1], [8]. However, if we set the power constraint as $\mathbb{E}[\mathbf{s}_{out}^H \mathbf{s}_{out}] \leq P_A$, then when $P_A \rightarrow 0$, i.e., there is no power supply at IRS, the amplification factor α_i will become 0. To ensure a fair comparison with the passive IRS, we subtract the received energy of the IRS from the amplification energy and formulate the constraint as in C2. Therefore, the total power consumed by the active IRS is $\mathbb{E}[\mathbf{s}_{out}^H \mathbf{s}_{out}] - \mathbb{E}[\mathbf{s}_{in}^H \mathbf{s}_{in}]$.

Note that \mathcal{P}_1 is very challenging to solve for two reasons. Firstly, the objective function is the expectation over a log determinant. Secondly, the objective function is the difference between two terms and the constraints C1 and C2 are coupled, making the optimization problem non-convex. In the following, we first derive the DA to approximate the normalized ergodic rate and then propose an effective AO-based algorithm to jointly optimize the transmit covariance matrix and the reflection matrix.

III. DETERMINISTIC APPROXIMATION OF ERGODIC RATE

Direct evaluation of the ergodic rate is very difficult. In this section, we first derive the DA for the normalized ergodic rate by leveraging RMT. For that purpose, we first introduce two important assumptions.

Assumption A-1. Let $c_1 = \frac{n_r}{n_t}$, $c_2 = \frac{n_l}{n_t}$, then $0 < \liminf c_1 \leq \limsup c_1 < +\infty$, $0 < \liminf c_2 \leq \limsup c_2 < +\infty$.

Assumption A-2. $\limsup_{\bar{n} \rightarrow +\infty} (\max_{i=1,2} \{\|\mathbf{R}_i\|, \|\tilde{\mathbf{T}}_i\|\}) < +\infty$.

A-1 implies that the number of transmit antennas, receive antennas, and active IRS elements grow to $+\infty$ at the same rate. In the following, we use $\bar{n} \rightarrow +\infty$ to represent this asymptotic regime. **A-2** implies that the antenna imbalance is finite [13].

For a positive measure μ over \mathbb{R} , its Stieltjes transform is defined as $m_\mu(z) = \int_{\mathbb{R}} \frac{\mu(dt)}{t-z}$, $z \in \mathbb{C} \setminus \text{supp}(\mu)$. We denote $\mathcal{S}(\mathbb{D})$ as the set of Stieltjes transforms for positive measures over domain \mathbb{D} . For matrix $\mathbf{M} \in \mathbb{C}^{n \times n}$, we denote $\mathbf{Q}_{\mathbf{M}}(z) = (-z\mathbf{I} + \mathbf{M})^{-1}$ as its resolvent matrix and $m_{\mathbf{M}}(z) = \frac{1}{n} \text{Tr} \mathbf{Q}_{\mathbf{M}}(z)$ represents the Stieltjes transform of its empirical spectrum distribution (ESD). In order to evaluate (5), we use the Shannon transform [14], i.e., $R(\mathbf{Q}, \Phi) = \int_{\sigma_s^2}^{+\infty} \mathbb{E}[m_{\mathbf{B}_2}(-t) - m_{\mathbf{B}_1}(-t)] dt$, where $m_{\mathbf{B}_1}(-t)$ and $m_{\mathbf{B}_2}(-t)$ are the Stieltjes transforms of the ESDs for \mathbf{B}_1 and \mathbf{B}_2 defined in (5). To approximate the ergodic rate, we first give the two DAs of $\mathbb{E}[m_{\mathbf{B}_1}(z)]$ and $\mathbb{E}[m_{\mathbf{B}_2}(z)]$ in the following two theorems.

Theorem 1. With assumptions **A-1** and **A-2**, we have

$$\mathbb{E}[m_{\mathbf{B}_1}(z)] - \frac{1}{n_r} \text{Tr}(-z\mathbf{I} + (\delta_2\delta_3 + \sigma_d^2\delta_4)\mathbf{R}_1)^{-1} \xrightarrow{\bar{n} \rightarrow +\infty} 0, \quad (7)$$

where δ_i , $i = 1, 2, 3, 4$, is the unique solution of the following system of equations

$$\delta_1 = \frac{1}{n_r} \text{Tr}[\mathbf{R}_1(-z\mathbf{I} + (\delta_2\delta_3 + \sigma_d^2\delta_4)\mathbf{R}_1)^{-1}], \quad (8)$$

$$\delta_2 = \frac{1}{n_l} \text{Tr}[\tilde{\mathbf{T}}_1^{\frac{1}{2}} \mathbf{R}_2 \tilde{\mathbf{T}}_1^{\frac{1}{2}} (\mathbf{I} + \sigma_d^2 c_1 \delta_1 \tilde{\mathbf{T}}_1 + c_1 \delta_1 \delta_3 \tilde{\mathbf{T}}_1^{\frac{1}{2}} \mathbf{R}_2 \tilde{\mathbf{T}}_1^{\frac{1}{2}})^{-1}], \quad (9)$$

$$\delta_3 = \frac{1}{n_t} \text{Tr}[\tilde{\mathbf{T}}_2 (\mathbf{I} + c_1 c_2 \delta_1 \delta_2 \tilde{\mathbf{T}}_2)^{-1}], \quad (10)$$

$$\delta_4 = \frac{1}{n_l} \text{Tr}[\tilde{\mathbf{T}}_1 (\mathbf{I} + \sigma_d^2 c_1 \delta_1 \tilde{\mathbf{T}}_1 + c_1 \delta_1 \delta_3 \tilde{\mathbf{T}}_1^{\frac{1}{2}} \mathbf{R}_2 \tilde{\mathbf{T}}_1^{\frac{1}{2}})^{-1}], \quad (11)$$

such that $\{\delta_1, \delta_1 \delta_2, \delta_1 \delta_3, \delta_1 \delta_4\} \subset \mathcal{S}(\mathbb{R}^+)$.

Proof: Please refer to Appendix A. ■

Theorem 2. *With assumptions A-1 and A-2, we have*

$$\mathbb{E}[m_{\mathbf{B}_2}(z)] - \frac{1}{n_r} \text{Tr}(-z\mathbf{I} + \alpha_2 \mathbf{R}_1)^{-1} \xrightarrow{\bar{n} \rightarrow +\infty} 0, \quad (12)$$

where α_i , $i = 1, 2$, is the unique solution of the following system of equations

$$\alpha_1 = \frac{1}{n_r} \text{Tr}[\mathbf{R}_1 (-z\mathbf{I} + \sigma_d^2 \alpha_2 \mathbf{R}_1)^{-1}], \quad (13)$$

$$\alpha_2 = \frac{1}{n_l} \text{Tr}[\tilde{\mathbf{T}}_1 (\mathbf{I} + c_1 \sigma_d^2 \alpha_1 \tilde{\mathbf{T}}_1)^{-1}], \quad (14)$$

such that $\{\alpha_1, -\frac{\alpha_2}{z}\} \subset \mathcal{S}(\mathbb{R}^+)$.

The proof of **Theorem 2** is similar to that of **Theorem 1** and is omitted here due to limited space. With the above two results, the DA for the normalized ergodic rate is given in the following theorem.

Theorem 3. $R(\mathbf{Q}, \Phi) - \bar{R}(\mathbf{Q}, \Phi) \xrightarrow{\bar{n} \rightarrow +\infty} 0$, where

$$\bar{R} = \bar{R}_1 - \bar{R}_2, \quad (15)$$

$$\begin{aligned} \bar{R}_1 = \frac{1}{n_r} & \left[\log \det(\mathbf{I} + \frac{\delta_2 \delta_3 + \sigma_d^2 \delta_4}{\sigma_s^2} \mathbf{R}_1) + \log \det(\mathbf{I} + c_1 c_2 \delta_1 \delta_2 \tilde{\mathbf{T}}_2) \right. \\ & \left. + \log \det(\mathbf{I} + c_1 \delta_1 \sigma_d^2 \tilde{\mathbf{T}}_1 + c_1 \delta_1 \delta_3 \tilde{\mathbf{T}}_1^{\frac{1}{2}} \mathbf{R}_2 \tilde{\mathbf{T}}_1^{\frac{1}{2}}) \right] - 2\delta_1 \delta_2 \delta_3 - \sigma_d^2 \delta_1 \delta_4, \end{aligned} \quad (16)$$

$$\bar{R}_2 = \frac{1}{n_r} \left[\log \det(\mathbf{I} + \frac{\sigma_d^2}{\sigma_s^2} \alpha_2 \mathbf{R}_1) + \log \det(\mathbf{I} + c_1 \sigma_d^2 \alpha_1 \tilde{\mathbf{T}}_1) \right] - \sigma_d^2 \alpha_1 \alpha_2. \quad (17)$$

Proof: Please refer to Appendix B. ■

Remark 2. *If we let $\sigma_d^2 \rightarrow 0$ in the fixed point system (8)-(11) and the DA of the normalized ergodic rate (15)-(17), δ_4 will disappear in \bar{R} and $\bar{R}_2 \rightarrow 0$. Moreover, if we let $a_i = 1$, the above result will degenerate to that in [4, Theorem 1] which is the DA for the normalized ergodic rate of passive IRS-aided MIMO systems.*

IV. OPTIMIZATION OF THE TRANSMIT COVARIANCE MATRIX AND THE REFLECTION MATRIX

Based on the DA derived in the last section, we develop an optimization algorithm for maximizing \bar{R} in this section. In particular, we reformulate the problem in (6) as

$$\begin{aligned} \mathcal{P}_2 : \quad & \underset{\mathbf{Q} \geq \mathbf{0}, \Phi}{\text{maximize}} \quad \bar{R}(\mathbf{Q}, \Phi) \\ & \text{s.t.} \quad \text{C1: } \text{Tr}(\mathbf{Q}) \leq n_t P_T, \\ & \quad \quad \text{C2: } \frac{\text{Tr}(\mathbf{Q}\mathbf{T}_2)}{n_t} \text{Tr}(\mathbf{R}_2(\Phi\Phi^H - \mathbf{I})) + \sigma_d^2 \text{Tr}(\Phi\Phi^H) \leq P_A. \end{aligned} \quad (18)$$

Since the constraints are coupled and \bar{R} is the difference between \bar{R}_1 and \bar{R}_2 , \mathcal{P}_2 is non-convex. To this end, we propose an AO-based algorithm to optimize \mathbf{Q} and Φ .

A. Optimization of the Transmit Covariance Matrix

For a given Φ , it can be shown that $\bar{R}(\mathbf{Q}, \Phi)$ is strictly concave with respect to \mathbf{Q} [4]. With the KKT condition, the original optimization problem \mathcal{P}_2 can be transformed into

$$\begin{aligned} \mathcal{P}_3 : \quad & \underset{\mathbf{Q} \geq \mathbf{0}}{\text{maximize}} \quad \mathcal{I}_1(\mathbf{Q}) = \frac{1}{n_r} \log \det(\mathbf{I} + c_1 c_2 \delta_1 \delta_2 \mathbf{Q}\mathbf{T}_2) \\ & \text{s.t.} \quad \text{C1: } \text{Tr}(\mathbf{Q}) \leq n_t P_T, \end{aligned} \quad (19)$$

and solved using the water filling method. The optimal solution is given by

$$\mathbf{Q}^{\text{opt}} = \mathbf{U}_{\mathbf{T}_2} \mathbf{\Lambda}_{\mathbf{Q}} \mathbf{U}_{\mathbf{T}_2}^H, \quad (20)$$

where $\mathbf{U}_{\mathbf{T}_2}$ is a unitary matrix whose columns are all eigenvectors of \mathbf{T}_2 , i.e., $\mathbf{T}_2 = \mathbf{U}_{\mathbf{T}_2} \mathbf{\Lambda}_{\mathbf{T}_2} \mathbf{U}_{\mathbf{T}_2}^H$. The eigenvalues of \mathbf{Q} is given by $\mathbf{\Lambda}_{\mathbf{Q}} = (\mu \mathbf{I} - (c_1 c_2 \delta_1 \delta_2 \mathbf{\Lambda}_{\mathbf{T}_2})^{-1})^+$, where μ is the parameter chosen to satisfy the constraint $\text{Tr}(\mathbf{Q}) \leq n_t P_T$.

B. Optimization the Reflection Matrix

For a given \mathbf{Q} , the optimization of Φ can be rewritten as

$$\begin{aligned} \mathcal{P}_4 : \quad & \underset{\Theta, \mathbf{A} \geq \mathbf{0}}{\text{maximize}} \quad \mathcal{I}_2(\Theta, \mathbf{A}) = \frac{1}{n_r} \left(-\log \det(\mathbf{I} + \mathbf{F}_2 \mathbf{A}^2) + \log \det(\mathbf{I} + \mathbf{F}_1 e^{-j\Theta} \mathbf{A} \mathbf{T}_1 \mathbf{A} e^{j\Theta}) \right) \\ & \text{s.t.} \quad \widehat{\text{C2:}} \quad \frac{\text{Tr}(\mathbf{Q}\mathbf{T}_2)}{n_t} \text{Tr}(\mathbf{R}_2(\mathbf{A}^2 - \mathbf{I})) + \sigma_d^2 \text{Tr}(\mathbf{A}^2) \leq P_A, \\ & \quad \quad \text{C3: } \mathbf{A} = \text{diag}\{a_1, a_2, \dots, a_{n_i}\}, \forall i, \\ & \quad \quad \text{C4: } \Theta = \text{diag}\{\theta_1, \theta_2, \dots, \theta_{n_i}\}, \theta_i \in [0, 2\pi), \forall i, \end{aligned} \quad (21)$$

where matrices \mathbf{F}_1 and \mathbf{F}_2 are defined as $\mathbf{F}_1 = (c_1\delta_1\sigma_d^2\mathbf{I} + c_1\delta_1\delta_3\mathbf{R}_2)$ and $\mathbf{F}_2 = c_1\sigma_d^2\alpha_1\mathbf{T}_1$, respectively. Moreover, we divide $\Phi = \mathbf{A}e^{j\Theta}$ into two parts with $\mathbf{A} = \text{diag}\{a_1, a_2, \dots, a_{n_l}\}$ and $e^{j\Theta} = \text{diag}\{e^{j\theta_1}, e^{j\theta_2}, \dots, e^{j\theta_{n_l}}\}$. The optimization problem with respect to Φ is non-convex due to the norm constraint of each element in $e^{j\Theta}$ and the difference of two log determinants in the objective function. The gradients for the divided parameters are, respectively, given by

$$\nabla_{\Theta}\mathcal{I}_2 = \frac{2}{n_r}\Im\left(\text{diag}\left\{(\mathbf{I} + \mathbf{F}_1\mathbf{M})^{-1}\right\}\right), \quad (22)$$

$$\nabla_{\mathbf{A}}\mathcal{I}_2 = \frac{2}{n_r}\Re\left(\text{diag}\left\{(\mathbf{A} + \mathbf{F}_2\mathbf{A}^3)^{-1} - (\mathbf{A} + \mathbf{A}\mathbf{F}_1\mathbf{M})^{-1}\right\}\right), \quad (23)$$

where $\mathbf{M} = e^{-j\Theta}\mathbf{A}\mathbf{T}_1\mathbf{A}e^{j\Theta}$. We denote the total parameter matrix by $\Omega = [\Theta, \mathbf{A}]$, such that the gradient can be rewritten as $\nabla_{\Omega}\mathcal{I}_2 = [\nabla_{\Theta}, \nabla_{\mathbf{A}}]$. Here, we adopt the backtracking line search method [15]. To start with, we define the constraint set of the optimization problem \mathcal{P}_4 as \mathcal{Q} . For a given $\tilde{\Omega}$, we denote the Euclid project operator by

$$\mathcal{P}_{\mathcal{Q}}(\tilde{\Omega}) = \arg \min_{\Omega \in \mathcal{Q}} \|\Omega - \tilde{\Omega}\|_F. \quad (24)$$

Assuming that the total parameter at the t -th iteration is $\Omega^{(t)} = [\Theta^{(t)}, \mathbf{A}^{(t)}]$, we search the best step size according to the following equation

$$\gamma^* = \arg \max_{\gamma \in [0, U]} \mathcal{I}_2(\mathcal{P}_{\mathcal{Q}}(\Omega^{(t)} + \gamma \nabla_{\Omega}\mathcal{I}_2)), \quad (25)$$

where U is a hyperparameter. Then, we update the phase transition and amplification matrix by $\Omega^{(t+1)} = \mathcal{P}_{\mathcal{Q}}(\Omega^{(t)} + \gamma^* \nabla_{\Omega}\mathcal{I}_2)$.

The proposed algorithm is summarized in **Algorithm 1**. Note that for a given Φ , the solution \mathbf{Q} of the \mathcal{P}_3 is optimal due to the concavity. On the other hand, for a given \mathbf{Q} , the adopted gradient line search method in \mathcal{P}_4 will converge because the objective function of \mathcal{P}_4 is monotonically increasing. Therefore, the proposed AO-based algorithm is guaranteed to converge.

V. NUMERICAL RESULTS

In this section, we validate the accuracy of the DAs and the effectiveness of the proposed AO-based algorithm via numerical simulations. In the simulation, we adopt the following channel correlation matrix model [16]

$$[\mathbf{C}(\eta, \delta, d_s)]_{m,n} = \int_{-180}^{180} \frac{d\phi}{\sqrt{2\pi\delta^2}} e^{2\pi j d_s(m-n) \sin(\frac{\pi\phi}{180}) - \frac{(\phi-\eta)^2}{2\delta^2}}, \quad (26)$$

where m and n denote the indexes of antennas or IRS elements, d_s is the receive antenna spacing, ϕ represents the angular spread of the signal, η is the mean angle, and δ denotes the

Algorithm 1 AO-Based Algorithm

- 1: Set iteration time $t = 0$, convergence tolerance $0 < \delta \ll 1$ and upper bound of search area U and initialize the optimization variables $\mathbf{Q}^{(0)}$ and $\mathbf{\Omega}^{(0)} = [\mathbf{A}^{(0)}, \mathbf{\Theta}^{(0)}]$
 - 2: **repeat**
 - 3: Calculate $\delta_i, i = 1, \dots, 4, \alpha_1$ and α_2 according to (8)-(11), (13) and (14) for given $\mathbf{Q}^{(t)}$ and $\mathbf{\Omega}^{(t)}$
 - 4: Update the optimal $\mathbf{Q}^{(t+1)}$ according to (20)
 - 5: Calculate the gradient $\nabla_{\mathbf{\Omega}} \mathcal{I}_2(\mathbf{\Omega}^{(t)})$ based on (22) and (23)
 - 6: Obtain the optimal step size γ^* by solving (25)
 - 7: Update the parameter $\mathbf{\Omega}^{(t+1)} = \mathcal{P}_{\mathcal{Q}}(\mathbf{\Omega}^{(t)} + \gamma^* \nabla_{\mathbf{\Omega}} \mathcal{I}_2)$
 - 8: Set $t = t + 1$
 - 9: **until** $\frac{|\bar{R}^{(t)} - \bar{R}^{(t-1)}|}{|\bar{R}^{(t)}|} \leq \delta$
 - 10: **Output:** $\mathbf{Q}^{(t)}$ and $\mathbf{\Omega}^{(t)}$
-

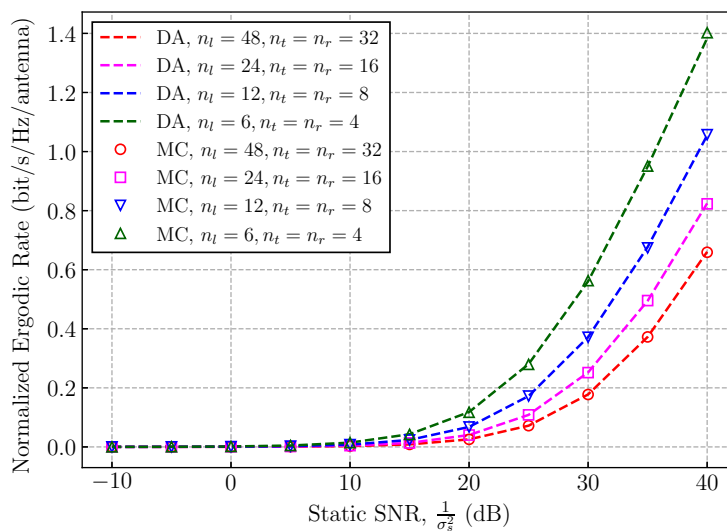


Fig. 2. The normalized ergodic rate versus signal to static noise ratio with $\sigma_d^2 = -30$ dBW. The dashed lines represent the DA analysis results.

root-mean-square angle spread. In the simulation, we set $\mathbf{T}_1 = \mathbf{C}(0, 30, 1)$, $\mathbf{T}_2 = \mathbf{C}(10, 5, 1)$, $\mathbf{R}_1 = \mathbf{C}(60, 30, 1)$, $\mathbf{R}_2 = \mathbf{C}(0, 30, 1)$. The path loss is set as $L_1 = L_2 = -25$ dB. The Monte-Carlo (MC) simulation results are illustrated by markers in all figures.

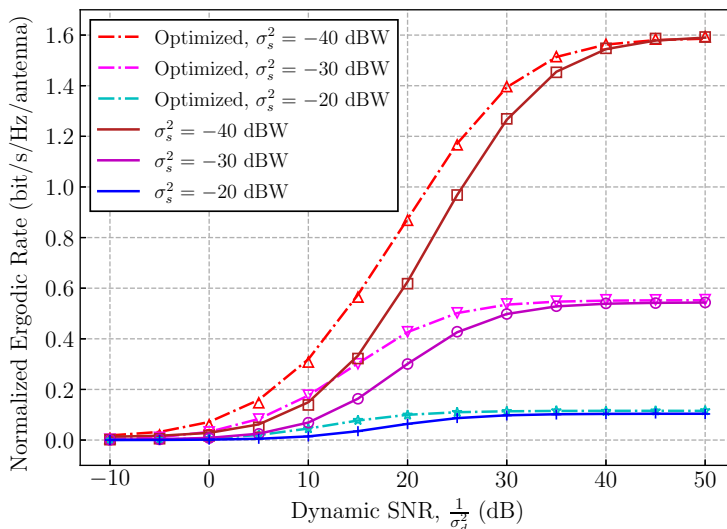


Fig. 3. The ergodic rate versus signal to dynamic noise ratio with $n_l = 18$, $n_t = n_r = 6$ and $P_T = P_A = 5$ W. The dash-dotted and solid lines represent the optimized and non-optimized results, respectively.

A. Accuracy of the DA

In Fig. 2, we compare the results of the DA analysis with MC simulation. In the experiment, we set $\sigma_d^2 = -30$ dBW, the number of antennas as $n_t = n_r \in \{4, 8, 16, 32\}$, and the number of elements of the active IRS as $n_l \in \{6, 12, 24, 48\}$. The MC simulation results are obtained by 5000 independent realizations of \mathbf{X}_1 and \mathbf{X}_2 in (2). As can be observed from Fig. 2, the approximation is very accurate even in the small dimensional setting ($n_l = 4$).

B. Effectiveness of the Proposed Algorithm

In Fig. 3, we show the effectiveness of the proposed algorithm with $n_l = 18$, $n_t = n_r = 6$ and $P_T = P_A = 5$ W. Comparing the solid and dash-dotted lines, we can observe that for a given σ_s^2 , the proposed algorithm is more effective when σ_d^2 is not too large or too small. Moreover, as the dynamic noise decreases, the ergodic rate will first grow and finally saturate. This can be explained by the fact that, as $\sigma_d^2 \rightarrow 0$, the ergodic rate is monotonically increasing and upper bounded, cf. (2).

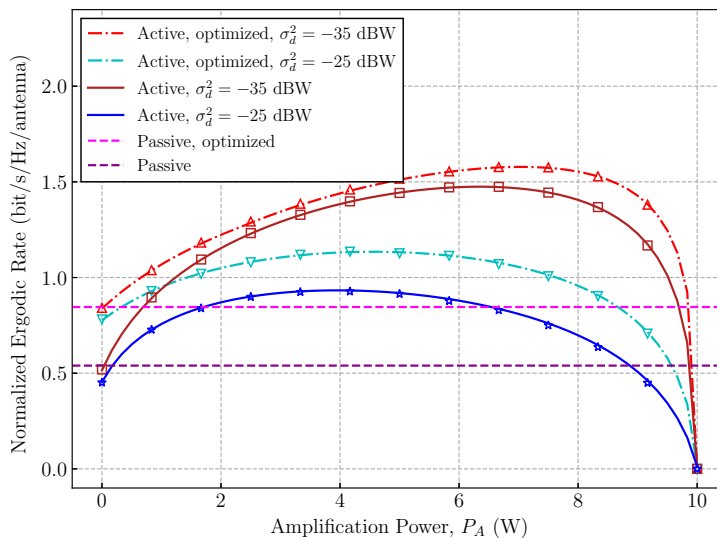


Fig. 4. The ergodic rate versus amplification power of the active IRS with $n_l = 12$, $n_t = n_r = 8$, $\sigma_s^2 = -40$ dBW and the total power $P_A + P_T = 10$ W. The dash-dotted and solid lines represent the optimized and non-optimized results of the active IRS, respectively. The dashed lines are optimized and non-optimized results of the passive IRS with $P_T = 10$ W.

C. Active IRS versus Passive IRS

To show the gain introduced by the active IRS, we compare its normalized ergodic rate with that of the passive IRS in Fig. 4. In the experiment, we set $n_l = 12$, $n_t = n_r = 8$ and $P_T + P_A = 10$ W for the active IRS and $P_T = 10$ W for the passive IRS. The static noises of two systems are set the same as $\sigma_s^2 = -40$ dBW. We have three observations from Fig. 4. First, as the power allocated to the active IRS increases, the optimized ergodic rate will increase at first and then decrease to 0. Recall the fact that the transmit signal will suffer from the “multiplicative fading” effect, but the signal amplified by the active IRS only goes through one hop, which avoids the severe path loss. As a result, when more power is allocated to the active IRS, the overall signal attenuation decreases, contributing to a rate improvement at the beginning. However, when the power of the transmitted signal is too small, the noise at the IRS will dominate the reflected signal, resulting in a significant performance degradation. Second, we can observe that the level of dynamic noise also influences the optimal power allocation policy. In fact, to increase the ergodic rate, more power should be allocated to the active IRS when the level of dynamic noise is not too high. Finally, even without optimization, the active IRS demonstrates its advantage

over its passive counterpart.

VI. CONCLUSION

In this paper, we investigated the benefit of using active IRSs in MIMO systems. For that purpose, we first derived the DA for the normalized ergodic rate, whose result was then utilized to jointly optimized the transmit covariance matrix and the reflection matrix, assuming only statistical CSI at the transmitter and the IRS. Numerical results validated the accuracy of the derived DA and the effectiveness of the proposed optimization algorithm. The analysis in this paper not only indicated that the active IRSs are a promising means to circumvent the “multiplicative fading” effect, but also unveiled their consistent advantages over the passive ones. Besides, when the level of dynamic noise is relatively low, it is advisable to allocate more energy to the active IRS.

APPENDIX A

PROOF OF THEOREM 1

To prove **Theorem. 1**, we first determine the DA of $\mathbb{E}[m_{\mathbf{B}_1}(z)]$ by the iterative method [5]. Then, we show the existence and uniqueness of the DA using the contraction mapping and the normal family argument [17].

To derive the DA, we use the iterative method, i.e., take the conditional expectation and integrate out the randomness of \mathbf{X}_i iteratively. Denote $\bar{\mathbf{T}}_1 = \tilde{\mathbf{T}}_1^{\frac{1}{2}}(\tilde{\mathbf{H}}_2\tilde{\mathbf{H}}_2^H + \sigma_d^2\mathbf{I})\tilde{\mathbf{T}}_1^{\frac{1}{2}}$. Based on [14, Theorem 1] with $K = 1$ and $\mathbf{S} = \mathbf{0}$ (due to the rotational invariance of Gaussian distribution, $\bar{\mathbf{T}}_1$ is not necessary diagonal), we can obtain the following relations

$$\alpha = \frac{1}{n_t} \text{Tr}[\mathbf{R}_1(-z\mathbf{I} + \tilde{\alpha}\mathbf{R}_1)^{-1}], \quad (27)$$

$$\tilde{\alpha} = \frac{1}{n_t} \text{Tr}[\bar{\mathbf{T}}_1(\mathbf{I} + \alpha\bar{\mathbf{T}}_1)^{-1}], \quad (28)$$

$$m_{\mathbf{B}_1}(z|\mathbf{X}_2) - \frac{1}{n_r} \text{Tr}(-z\mathbf{I} + \tilde{\alpha}\mathbf{R}_1)^{-1} \xrightarrow[\bar{n} \rightarrow +\infty]{a.s.} 0, \quad (29)$$

where $m_{\mathbf{B}_1}(z|\mathbf{X}_2) = \mathbb{E}[m_{\mathbf{B}_1}(z)|\mathbf{X}_2]$ is the conditional expectation. We define the resolvent matrix of $\bar{\mathbf{T}}_1$ by $\Upsilon(z) = (-z\mathbf{I} + \bar{\mathbf{T}}_1)^{-1} = (-z\mathbf{I} + \sigma_d^2\tilde{\mathbf{T}}_1 + \tilde{\mathbf{T}}_1^{\frac{1}{2}}\tilde{\mathbf{H}}_2\tilde{\mathbf{H}}_2^H\tilde{\mathbf{T}}_1^{\frac{1}{2}})^{-1}$ and denote $\tilde{\mathbf{R}}_2 = \tilde{\mathbf{T}}_1^{\frac{1}{2}}\mathbf{R}_2\tilde{\mathbf{T}}_1^{\frac{1}{2}}$. By referring to [14, Theorem 1] with $K = 1$ and $\mathbf{S} = \sigma_d^2\tilde{\mathbf{T}}_1$, we have

$$\beta = \frac{1}{n_t} \text{Tr}[\tilde{\mathbf{R}}_2(-z\mathbf{I} + \sigma_d^2\tilde{\mathbf{T}}_1 + \tilde{\beta}\tilde{\mathbf{R}}_2)^{-1}], \quad (30)$$

$$\tilde{\beta} = \frac{1}{n_t} \text{Tr}[\tilde{\mathbf{T}}_2(\mathbf{I} + \beta\tilde{\mathbf{T}}_2)^{-1}], \quad (31)$$

$$\mathbb{E}[m_{\tilde{\mathbf{T}}_1}(z)] - \frac{1}{n_l} \text{Tr}(-z\mathbf{I} + \sigma_d^2\tilde{\mathbf{T}}_1 + \tilde{\beta}\tilde{\mathbf{R}}_2)^{-1} \xrightarrow{\bar{n} \rightarrow +\infty} 0. \quad (32)$$

Now we deal with \mathbf{X}_2 in (29). Further derivation shows that

$$\begin{aligned} \tilde{\alpha} &= \frac{1}{n_l\alpha} \text{Tr}[\mathbf{I} - (\mathbf{I} + \sigma_d^2\alpha\tilde{\mathbf{T}}_1 + \tilde{\beta}\alpha\tilde{\mathbf{R}}_2)^{-1} \\ &\quad + (\mathbf{I} + \sigma_d^2\alpha\tilde{\mathbf{T}}_1 + \tilde{\beta}\alpha\tilde{\mathbf{R}}_2)^{-1} - \frac{1}{\alpha}\mathbf{r}(-\frac{1}{\alpha})] \\ &= \bar{\alpha} + o_{a.s.}(1), \end{aligned} \quad (33)$$

where $\bar{\alpha} = \sigma_d^2\gamma_\alpha + \frac{1}{c_2\alpha}\tilde{\beta}(-\frac{1}{\alpha})\beta(-\frac{1}{\alpha})$, $\gamma_\alpha = \frac{1}{n_l} \text{Tr}[\tilde{\mathbf{T}}_1(\mathbf{I} + \sigma_d^2\alpha\tilde{\mathbf{T}}_1 + \tilde{\beta}\alpha\tilde{\mathbf{R}}_2)^{-1}]$ and $o_{a.s.}(1)$ is a r.v. that almost surely converges to 0. By denoting $[\delta_1, \delta_2, \delta_3, \delta_4] = [\frac{\alpha}{c_1}, \frac{\beta}{\alpha c_2}, \tilde{\beta}, \gamma_\alpha]$, we can obtain (8)-(11). By the almost sure convergence of (29) and the dominated convergence theorem, we have

$$\mathbb{E}[m_{\mathbf{B}_1}(z|\mathbf{X}_2)] - \frac{1}{n_r} \text{Tr}(-z\mathbf{I} + \bar{\alpha}\mathbf{R}_1)^{-1} \xrightarrow{\bar{n} \rightarrow +\infty} 0, \quad (34)$$

which proves (7) in **Theorem. 1**.

Next we will prove the existence of the system of equations. For notational simplicity, we define $\Psi^{(0)}$ as $\Psi^{(0)} = [\psi_1^{(0)}, \psi_2^{(0)}, \psi_3^{(0)}, \psi_4^{(0)}] = [\delta_1^{(0)}, \delta_1^{(0)}\delta_2^{(0)}, \delta_1^{(0)}\delta_3^{(0)}, \delta_1^{(0)}\delta_4^{(0)}] = -\frac{1}{z}\mathbf{1}_4^T$. Plugging $\Psi^{(i)}$ in the system of equations, we can get $\Psi^{(i+1)}$. Furthermore, we can prove by induction that

- i) $\psi_k^{(i)}, \bar{\psi}^{(i)} \in \mathcal{S}(\mathbb{R}^+)$, where $\bar{\psi}^{(i)} = -\frac{\psi_2^{(i)}\psi_3^{(i)}}{z(\psi_1^{(i)})^2} - \frac{\sigma_d^2\psi_4^{(i)}}{z\psi_1^{(i)}}$.
- ii) for $z < 0$, $0 \leq \psi_k^{(i)}, \bar{\psi}^{(i)} \leq \frac{K}{|z|}$, where K is a constant.

To prove that a function $\psi \in \mathcal{S}(\mathbb{R}^+)$, we need to validate that $\Im(\psi(z)) > 0$ for $z \in \mathbb{C}^+$, ψ is analytic over \mathbb{C}^+ and $\lim_{y \rightarrow +\infty} -jy\psi(jy)$ converges [17]. Due to the limited space, we only discuss $\psi_1^{(i)}$ here and the rest are similar. Let $\bar{\mathbf{Q}}^{(i)} = -\frac{1}{z}(\mathbf{I} + \bar{\psi}^{(i)}\mathbf{R}_1)^{-1}$, $\mathcal{E}^{(i)} = \max_{k \in \{1,2,3,4\}} \{|\psi_k^{(i)} - \psi_k^{(i-1)}|, |\bar{\psi}^{(i)} - \bar{\psi}^{(i-1)}|\}$. For $z < 0$, we have

$$\begin{aligned} |\psi_1^{(i+1)} - \psi_1^{(i)}| &\leq |z| |\bar{\psi}^{(i)} - \bar{\psi}^{(i-1)}| \\ &\quad \times \left| \frac{1}{n_r} \text{Tr}(\mathbf{R}_1\bar{\mathbf{Q}}^{(i)}\mathbf{R}_1\bar{\mathbf{Q}}^{(i-1)}) \right| \\ &\leq \|\mathbf{R}_1\|^2 \frac{1}{|z|} \mathcal{E}^{(i)} = \frac{K_1}{|z|} \mathcal{E}^{(i)}, \end{aligned} \quad (35)$$

where K_1 is a constant that is independent of z . Similarly, we have $\mathcal{E}^{(i+1)} \leq \frac{K_{1,2,3,4}}{|z|} \mathcal{E}^{(i)}$. For $z < -C$ with $C > 0$ large enough, $\psi_k^{(i)}(z)$ forms a Cauchy sequence. So $\psi_k^{(i)}(z)$ has a unique limit denoted by $\psi_k(z)$ for $z < -C$. $\psi_k^{(i)} \in \mathcal{S}(\mathbb{R}^+)$, so $\psi_k^{(i)}$ is analytic and uniformly bounded on

each compact subset of $\mathbb{C} \setminus \mathbb{R}^+$. According to the normal family theorem [18], ψ_k is analytic on $\mathbb{C} \setminus \mathbb{R}^+$. Finally, $\psi_k \in \mathcal{S}(\mathbb{R}^+)$ can be proved by verifying that $\lim_{y \rightarrow +\infty} -jy\psi_k(jy)$ converges. The uniqueness of ψ_k can be proved in the same way, i.e., assuming there exist two solutions ψ_k and $\tilde{\psi}_k$ both in $\mathcal{S}(\mathbb{R}^+)$, we can perform the subtraction like (35) to find the contraction. Therefore we complete the proof of **Theorem 1**. ■

APPENDIX B

PROOF OF THEOREM 3

Denoting $t = \sigma_s^2$ in \bar{R}_1 , we can get $\frac{\partial \bar{R}_1}{\partial t} = \sum_i \frac{\partial \bar{R}_1}{\partial \delta_i} \frac{\partial \delta_i}{\partial t} + \frac{1}{n_r} \text{Tr}(t\mathbf{I} + (\delta_2\delta_3 + \sigma_d^2\delta_4)\mathbf{R}_1)^{-1} - \frac{1}{t}$. It can be shown that (due to space limitations, the proof is omitted here) δ_i is bounded for $t \geq \sigma_s^2$, i.e., $\delta_i \in [c, C]$, where $c \geq 0$ and $C > 0$ are constants. So $\lim_{t \rightarrow +\infty} \bar{R}_1(t) = 0$. Simple derivations show that $\frac{\partial \bar{R}_1}{\partial \delta_i} = 0$. Thus $\frac{\partial \bar{R}_1(t)}{\partial t}$ is bounded and integrable for $t \in [\sigma_s^2, +\infty)$ and we have

$$\begin{aligned} \bar{R}_1 &= \int_{\sigma_s^2}^{+\infty} -\frac{\partial \bar{R}_1}{\partial t} dt \\ &= \int_{\sigma_s^2}^{+\infty} \frac{1}{t} - \frac{1}{n_r} \text{Tr}(t\mathbf{I} + (\delta_2\delta_3 + \sigma_d^2\delta_4)\mathbf{R}_1)^{-1} dt \\ &= \int_{\sigma_s^2}^{+\infty} \frac{1}{t} - \mathbb{E}[m_{\mathbf{B}_1}(-t)] dt + o(1), \end{aligned} \quad (36)$$

where $o(1)$ is a deterministic term that converges to zero. The same method can be applied to \bar{R}_2 . Thus, we complete the proof. ■

REFERENCES

- [1] Q. Wu and R. Zhang, "Intelligent reflecting surface enhanced wireless network via joint active and passive beamforming," *IEEE Trans. Wireless Commun.*, vol. 18, no. 11, pp. 5394–5409, Aug. 2019.
- [2] C. Huang, A. Zappone, G. C. Alexandropoulos, M. Debbah, and C. Yuen, "Reconfigurable intelligent surfaces for energy efficiency in wireless communication," *IEEE Trans. Wireless Commun.*, vol. 18, no. 8, pp. 4157–4170, Jun. 2019.
- [3] S. Zhang and R. Zhang, "Capacity characterization for intelligent reflecting surface aided MIMO communication," *IEEE J. Sel. Areas Commun.*, vol. 38, no. 8, pp. 1823–1838, Jun. 2020.
- [4] J. Zhang, J. Liu, S. Ma, C.-K. Wen, and S. Jin, "Transmitter design for large intelligent surface-assisted MIMO wireless communication with statistical CSI," in *Proc. Int. Conf. Commun. Wkshps. (ICC Wkshps)*, Dublin, Ireland, Jun. 2020, pp. 1–5.
- [5] X. Zhang, X. Yu, S. Song, and K. B. Letaief, "IRS-aided MIMO systems over double-scattering channels: Impact of channel rank deficiency," in *Proc. IEEE Wireless Commun. Netw. Conf. (WCNC)*, Austin, TX, USA, Apr. 2022, pp. 2076–2081.
- [6] Q.-U.-A. Nadeem, A. Zappone, and A. Chaaban, "Intelligent reflecting surface enabled random rotations scheme for the MISO broadcast channel," *IEEE Tran. Wireless Commun.*, vol. 20, no. 8, pp. 5226–5242, Mar. 2021.

- [7] M. Najafi, V. Jamali, R. Schober, and H. V. Poor, "Physics-based modeling of large intelligent reflecting surfaces for scalable optimization," in *Proc. IEEE 54nd Asilomar Conf. Signals, Syst., Comput.*, Pacific Grove, CA, USA, Oct. 2020, pp. 559–563.
- [8] Z. Zhang, L. Dai, X. Chen, C. Liu, F. Yang, R. Schober, and H. V. Poor, "Active RIS vs. passive RIS: Which will prevail in 6G?" *IEEE Trans. Commun.*, vol. 71, no. 3, pp. 1707–1725, Mar. 2023.
- [9] C. You and R. Zhang, "Wireless communication aided by intelligent reflecting surface: Active or passive?" *IEEE Wireless Commun. Lett.*, vol. 10, no. 12, pp. 2659–2663, Sep. 2021.
- [10] K. Zhi, C. Pan, H. Ren, K. K. Chai, and M. ElKashlan, "Active RIS versus passive RIS: Which is superior with the same power budget?" *IEEE Commun. Lett.*, vol. 26, no. 5, pp. 1150–1154, Mar 2022.
- [11] G. Zhou, C. Pan, H. Ren, D. Xu, Z. Zhang, J. Wang, and R. Schober, "A framework for transmission design for active RIS-aided communication with partial CSI," *arXiv:2302.09353*, 2023.
- [12] D. Xu, X. Yu, D. W. Kwan Ng, and R. Schober, "Resource allocation for active IRS-assisted multiuser communication systems," in *Proc. IEEE 55nd Asilomar Conf. Signals, Syst., Comput.*, Pacific Grove, CA, USA, Oct. 2021, pp. 113–119.
- [13] X. Zhang and S. Song, "Bias for the trace of the resolvent and its application on non-gaussian and non-centered MIMO channels," *IEEE Trans. Inf. Theory*, vol. 68, no. 5, pp. 2857–2876, Dec. 2021.
- [14] R. Couillet, M. Debbah, and J. W. Silverstein, "A deterministic equivalent for the analysis of correlated MIMO multiple access channels," *IEEE Trans. Inf. Theory*, vol. 57, no. 6, pp. 3493–3514, May 2011.
- [15] S. Boyd and L. Vandenberghe, *Convex Optimization*. Cambridge university press, 2004.
- [16] A. Moustakas, S. Simon, and A. Sengupta, "MIMO capacity through correlated channels in the presence of correlated interferers and noise: a (not so) large N analysis," *IEEE Trans. Inf. Theory*, vol. 49, no. 10, pp. 2545–2561, Oct. 2003.
- [17] W. Hachem, P. Loubaton, and J. Najim, "Deterministic equivalents for certain functionals of large random matrices," *Ann. Appl. Probab.*, no. 3, pp. 875–930, Jun. 2007.
- [18] W. Rudin, *Real and Complex Analysis*. McGraw-Hill, New York, 1987.